Publication Year	2016
Acceptance in OA@INAF	2020-05-20T16:06:33Z
Title	INTEGRAL study of temporal properties of bright flares in Supergiant Fast X-ray Transients
Authors	SIDOLI, Lara; PAIZIS, ADAMANTIA; Postnov, K.
DOI	10.1093/mnras/stw237
Handle	http://hdl.handle.net/20.500.12386/25018
Journal	MONTHLY NOTICES OF THE ROYAL ASTRONOMICAL SOCIETY
Number	457

Monthly Notices
of the
ROYAL ASTRONOMICAL SOCIETY

MNRAS **457,** 3693–3701 (2016) doi:10.1093/mnras/stw237
Advance Access publication 2016 January 29

INTEGRAL study of temporal properties of bright flares in Supergiant Fast X-ray Transients

L. Sidoli,[1]★ A. Paizis[1] and K. Postnov[2,3]

[1]*INAF, Istituto di Astrofisica Spaziale e Fisica Cosmica, Via E. Bassini 15, I-20133 Milano, Italy*
[2]*Faculty of Physics, Moscow Lomonosov State University, Leninskie Gory 1, 117234 Moscow, Russia*
[3]*Sternberg Astronomical Institute, Moscow Lomonosov State University, 117234 Moscow, Russia*

Accepted 2016 January 26. Received 2016 January 25; in original form 2015 December 15

ABSTRACT

We have characterized the typical temporal behaviour of the bright X-ray flares detected from the three Supergiant Fast X-ray Transients (SFXTs) showing the most extreme transient behaviour (XTE J1739−302, IGR J17544−2619, SAX J1818.6−1703). We focus here on the cumulative distributions of the waiting-time (time interval between two consecutive X-ray flares), and the duration of the hard X-ray activity (duration of the brightest phase of an SFXT outburst), as observed by *INTEGRAL*/IBIS in the energy band 17–50 keV. Adopting the cumulative distribution of waiting-times, it is possible to identify the typical time-scale that clearly separates different outbursts, each composed by several single flares at ∼ks time-scale. This allowed us to measure the duration of the brightest phase of the outbursts from these three targets, finding that they show heavy-tailed cumulative distributions. We observe a correlation between the total energy emitted during SFXT outbursts and the time interval covered by the outbursts (defined as the elapsed time between the first and the last flare belonging to the same outburst as observed by *INTEGRAL*). We show that temporal properties of flares and outbursts of the sources, which share common properties regardless different orbital parameters, can be interpreted in the model of magnetized stellar winds with fractal structure from the OB-supergiant stars.

Key words: stars: neutron – X-rays: binaries – X-rays: individuals: XTE J1739−302, IGR J17544−2619, SAX J1818.6−1703.

1 INTRODUCTION

Supergiant Fast X-ray Transients (SFXTs; Sguera et al. 2005; Negueruela et al. 2006) are a subclass of high-mass X-ray binaries (HMXBs) that was unveiled after the discovery by the *INTEGRAL* satellite of many short hard X-ray transients in the Galactic plane (the first *INTEGRAL* source of this class was discovered by Sunyaev et al. 2003).

SFXTs host a neutron star (NS, hereafter) accreting from the wind of either an O or B-type supergiant and display rare outbursts punctuated by short (∼1–2 ks) luminous flares reaching 10^{36}–10^{37} erg s^{-1}, characterized by a duty cycle lower than a few per cent (Lutovinov et al. 2013; Paizis & Sidoli 2014, hereafter PS14; Romano et al. 2014a). When observed at softer X-rays (1–10 keV) with more sensitive instruments, SFXTs are caught at X-ray luminosities below 10^{34} erg s^{-1} most of the time (Sidoli et al. 2008; Romano et al. 2014b; Bozzo et al. 2015). In some members of the class, a luminosity as low as 10^{32} erg s^{-1} (1–10 keV) has been observed, leading to a very high observed dynamic range (ratio between luminosity during outburst and quiescence) up to six orders of magnitude, in the most extreme case of the SFXT IGR J17544−2619 (in't Zand 2005; Romano et al. 2015).

The mechanism responsible for the SFXT flaring behaviour, associated with the accretion on to the NS by a fraction of the donor wind, has been discussed by many authors. Some of them explain the SFXT flares with the particular properties of the compact object (e.g. propeller effect or magnetic gating mechanism; Grebenev & Sunyaev 2007; Bozzo, Falanga & Stella 2008), others invoke a variety of orbital geometries together with the clumpy properties of the wind of the massive star (in't Zand 2005; Sidoli et al. 2007; Walter & Zurita Heras 2007; Negueruela et al. 2008; Ducci et al. 2009). More recently, an alternative model has been proposed to explain bright flares in SFXTs (Shakura et al. 2014), based on the instability of the quasi-spherical shell of captured matter which accumulates above the magnetosphere of a slowly rotating NS at low accretion rates (Shakura et al. 2012).

After more than 10 yr from the discovery of SFXTs with *INTEGRAL*, the *INTEGRAL*/IBIS public archive is providing us with an observational data set of X-ray flares detected from SFXTs

★ E-mail: sidoli@lambrate.inaf.it

© 2016 The Authors
Published by Oxford University Press on behalf of the Royal Astronomical Society

Downloaded from https://academic.oup.com/mnras/article-abstract/457/4/3693/2589033 by guest on 06 May 2020

that is large enough to enable a statistical investigation. PS14 have exploited the *INTEGRAL* archive, investigating the cumulative distributions of the hard X-ray luminosity (17–100 keV) of SFXT flares, finding that they follow a power-law distribution, completely different with respect to the lognormal luminosity distribution shown by the emission from persistent 'classical' HMXBs (e.g. Vela X−1). These SFXT properties were successfully interpreted by PS14 and Shakura et al. (2014) in terms of the model of unstable settling accretion on to slowly rotating magnetized NS (Shakura et al. 2012).

Here, we investigate other important properties of the same sample of SFXT flares reported by PS14: the waiting-time (WT) between two consecutive flares and the duration of the brightest phase of the outbursts, as observed by *INTEGRAL*, in order to get more insights into the nature of these transients. We refer to PS14 for the summary of the SFXT properties adopted in this paper.

2 DATA ANALYSIS

We focus here on the hard X-ray flares caught by *INTEGRAL*/IBIS observations covering about 9 yr, from 2002 December to 2012 April (see PS14). In this work, we consider the three SFXTs which show the highest dynamic range (XTE J1739−302, IGR J17544−2619, and SAX J1818.6−1703) and are often referred to as 'prototypical SFXTs' in the literature.

Data selection and analysis have already been reported by PS14, adopting the data reduction procedure described in detail by Paizis et al. (2013). We refer the reader to these papers for the technical details. In brief, the data sets of detected X-ray flares consist of all IBIS pointing images (the so-called Science Windows, hereafter ScWs, with a typical exposure time of ∼2 ks) where the sources were within 12° from the image centre and found to be active (detection significance $>5\sigma$). Therefore, in this work we use the image deconvolution results (IMA results) as reported by PS14. As already discussed in PS14, since the typical time-scale of flare duration is consistent with an ScW exposure time, we consider that a single IBIS/ISGRI detection on ScW level is representative of an SFXT flare.

The characterization of the luminosity distributions in hard X-rays of the SFXT flares and their energy release have been already discussed by PS14 and Shakura et al. (2014), respectively.

In this work, we consider the same data set of X-ray flares selected and reported by PS14 for the three sources XTE J1739−302, IGR J17544−2619, and SAX J1818.6−1703, with the aim of further characterizing their temporal properties.

3 RESULTS

We consider the light curves of the X-ray flares (luminosity is in the energy band 17–50 keV) detected from the three SFXTs during *INTEGRAL*/IBIS observations spanning about 9 yr. Typical light curves during SFXT outbursts are shown in Fig. 1 (where each detection corresponds to a flare on ScW time-scale). We define WT between two consecutive flares, the difference between the start times of two subsequent ScWs where an SFXT flare is detected. The shortest WT corresponds to the duration of an ScW (in case of flares detected in adjacent ScWs). In Fig. 2, we show the cumulative distribution of WTs between 'consecutive' flares, for each of the three targets.

The highly populated vertical lines in Fig. 2, corresponding to the shortest WT (below 0.1 d), are produced by flares detected in adjacent ScWs. At the opposite side of the *x*-axis, WTs larger than 100 d might be significantly affected by the data gaps between two

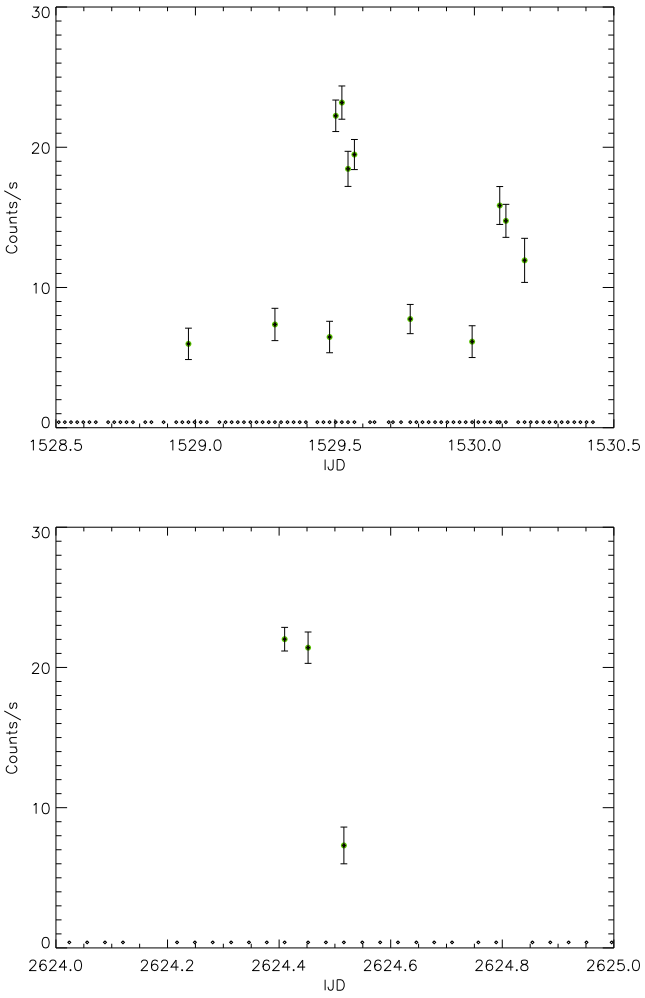

Figure 1. Examples of SFXT light curves during outbursts (XTE J1739−302), as observed by *INTEGRAL* (17–50 keV): a longer (upper panel) and a shorter outburst (lower panel). Time is in units of *INTEGRAL* day (IJD = MJD – 51544). Diamonds along the *x*-axis mark the times of the *INTEGRAL* observations (ScWs) of the source field, while the solid green circle represents the detections, i.e. the X-ray flares (the source count rate has been extracted over a ScW time-scale, see text). The upper panel clearly shows the difference between two time-scales defined in the text (the total duration '*D*' of the active phase of this outburst is 16 ks, while the elapsed time 'Δt' between the last and the first flare of the same outburst is 10^5 s; see text for details).

satellite visibility windows of the source sky position, as suggested by the steepening of the WT distribution above 100 d, particularly evident in XTE J1739−302 and IGR J17544−2619. Other biases due to gaps in the data are unlikely to severely affect the shape of the true distribution at intermediate WTs (between a few days and 100 d), given the low duty cycles of these three SFXTs.

An interesting feature present in all three WT distributions is a plateau just above ∼1 d (i.e. missing WTs in that temporal range). This strongly suggests that a WT of ∼1 d (1.4 d, to be precise, in order to include the last point of the plateau in SAX J1818.6−1703) can be adopted as a time-scale to separate the flaring activity belonging to two different and subsequent outbursts (each composed by a cluster of many flares).

This makes it possible to derive the time duration of single outbursts and to study their statistical properties (e.g. cumulative distribution) and correlations. In order to determine the total duration

Downloaded from https://academic.oup.com/mnras/article-abstract/457/4/3693/2589033 by guest on 06 May 2020

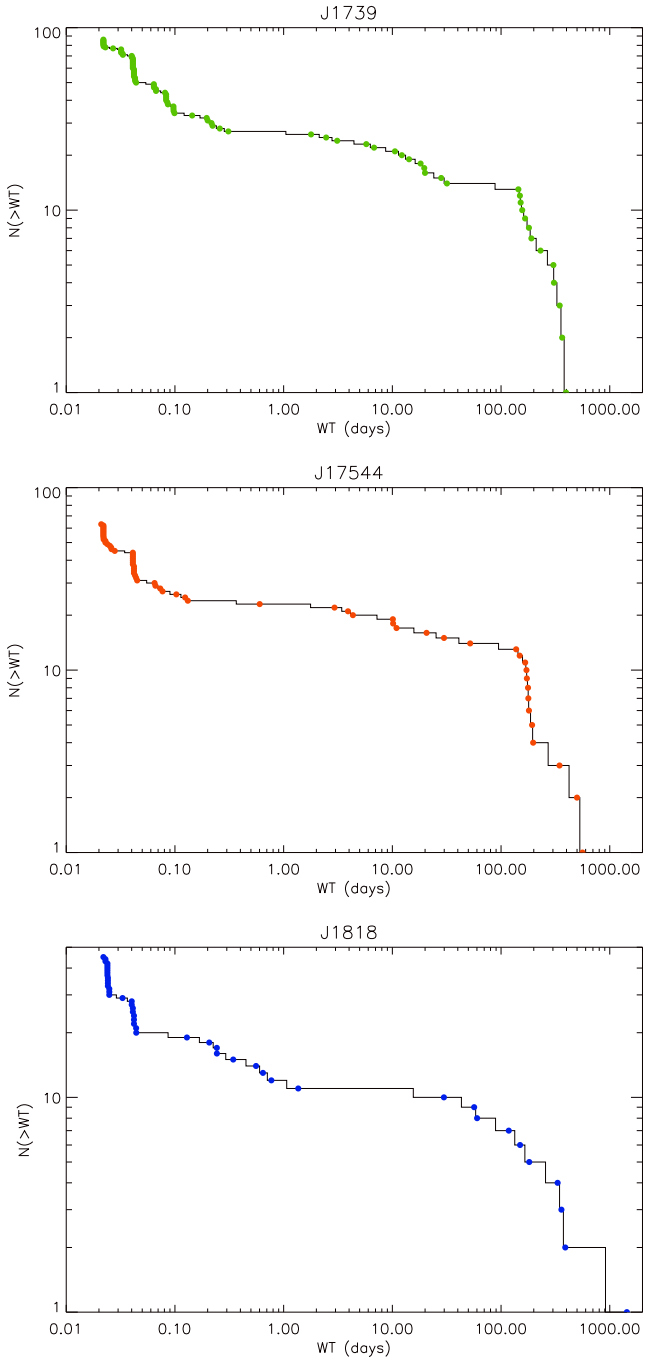

Figure 2. Cumulative distributions of the WT between two consecutive bright flares in the three SFXTs as observed by *INTEGRAL*/IBIS in about 9 yr of data (17–50 keV).

of a bright X-ray flaring activity episode (a single outburst) as observed by *INTEGRAL*/IBIS, we adopt the following procedure: for each SFXT, we start from the second X-ray flare detected in the *INTEGRAL*/IBIS light curve and calculate its WT with respect to the first flare. If this WT is lower than 1 d, then the flare is assumed to belong to the same bright outburst phase as the previous flare. Performing this comparison with the following flares, at one point there will be a flare for which the WT with respect to the immediately previous flare is greater than 1 d. At this point the procedure stops and a list of clusters of flares (i.e. outburst) is produced for the three SFXTs.

This automatic process has led to the empirical determination of the duration of the SFXTs outbursts, as observed by *INTEGRAL*. To do this, we defined two different temporal quantities: the *total duration* (D) of the brightest phase of an outburst and the *elapsed time interval* (Δt) between the first and the last flare belonging to an outburst (see Fig. 1, upper panel and caption, for an example). More in detail: for each source, for each single outburst, we calculated the total duration (D) simply by adding together the durations, d_i, of single flares belonging to the same outburst ($D = \sum_{i=1}^{N} d_i$, where N is the number of flares in a single outburst). Since the flares composing an outburst can be either detected in adjacent pointings or not, D can be interpreted as the integrated time each SFXT spends in its brightest state during a single outburst as observed by IBIS. Durations D lower than 2–3 ks imply that only one isolated flare is caught by *INTEGRAL* during a supposed (although unobserved) longer outburst. Very likely, these single flares represent the brightest activity of outbursts with average fainter luminosity, where *INTEGRAL* detects only the brightest part.

Another temporal quantity that can be calculated from the light curves of X-ray flares, for each outburst, is the elapsed time interval, Δt (where $\Delta t = \mathrm{tstop}_N - \mathrm{tstart}_1$) between the first (1) and the last (N) flare belonging to the same outburst (as previously defined).

3.1 Cumulative distributions

The cumulative distributions of the durations D of the brightest phase in each single outburst for the three SFXTs considered here are shown in Fig. 3. In particular, an evident flattening at short durations is present in the IGR J17544−2619 duration distribution, due to single flares. While the cumulative distribution of the outburst duration in SAX J1818.6−1703 appears to be exponential, in the case of IGR J17544−2619 and XTE J1739−302, if we exclude the flatter region at low duration composed by single flares, they are power-law-like. Adopting a maximum-likelihood estimation of the power-law slope (PS14) from a subsample of data points above a truncation point of 2 and 3 ks (respectively, for XTE J1739−302 and IGR J17544−2619), we obtained a power-law slope, β, of 1.6±0.6 able to adequately describe the cumulative distribution outburst duration in IGR J17544−2619, while $\beta = 0.5 \pm 0.2$ in XTE J1739−302. We note that in all three SFXTs, the cumulative distribution of the total durations of the outburst phases (in their brightest phase, the one that IBIS is able to detect) display a cut-off above 10 ks. In particular, the maximum outburst durations observed in our data set are 13 ks in SAX J1818.6−1703, 26 ks in IGR J17544−2619 and 29 ks in XTE J1739−302.

The distributions of the elapsed times, Δt, for the three SFXTs are shown in Fig. 4. Note that in case of outbursts made of a single isolated flare, again, Δt is equal to the duration of the single flare. This causes the flattening of the distributions at low Δt around 1–2 ks (and below). Above this time-scale, the distribution of Δt in XTE J1739−302 shows a steepening (higher frequency of flares) around 5–6 ks, with a few outbursts composed by only 2–3 flares, while above 10 ks the cumulative distribution is power-law-like. In IGR J17544−2619, a power-law-like distribution of Δt is present above around 5–6 ks, while in SAX J1818.6−1703 a roll-over above about 30–40 ks emerges.

In Fig. 5, we show the cumulative distribution of the total durations (D_{all}, upper panel) and elapsed times (Δt_{all}, lower panel), respectively, taken from combining time-scales characterizing the outbursts from all three SFXTs. It is remarkable that a power-law distribution is able to adequately describe the global behaviour of the three prototypical SFXTs, with slopes, β, of 0.9±0.3 and 0.3±0.1

Downloaded from https://academic.oup.com/mnras/article-abstract/457/4/3693/2589033 by guest on 06 May 2020

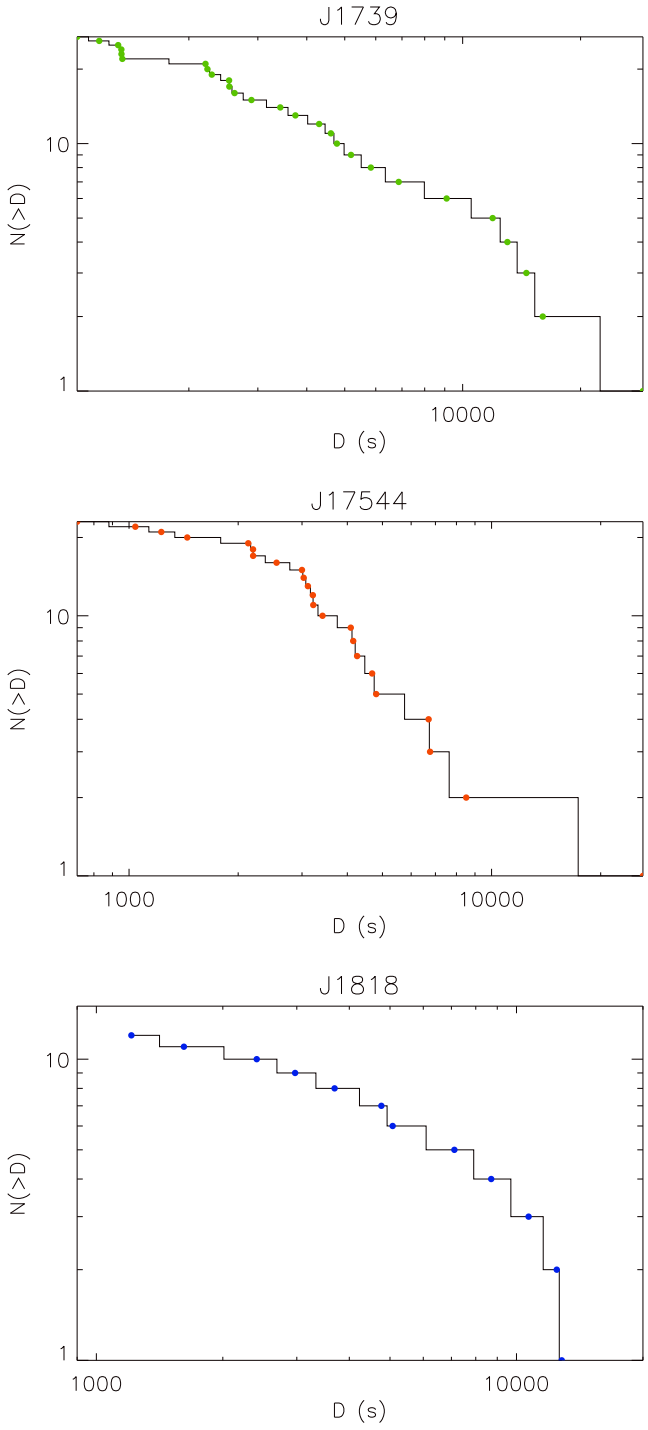

Figure 3. Cumulative distributions of the duration (D) of the outbursts in the three SFXTs, as observed by *INTEGRAL*/IBIS (17–50 keV).

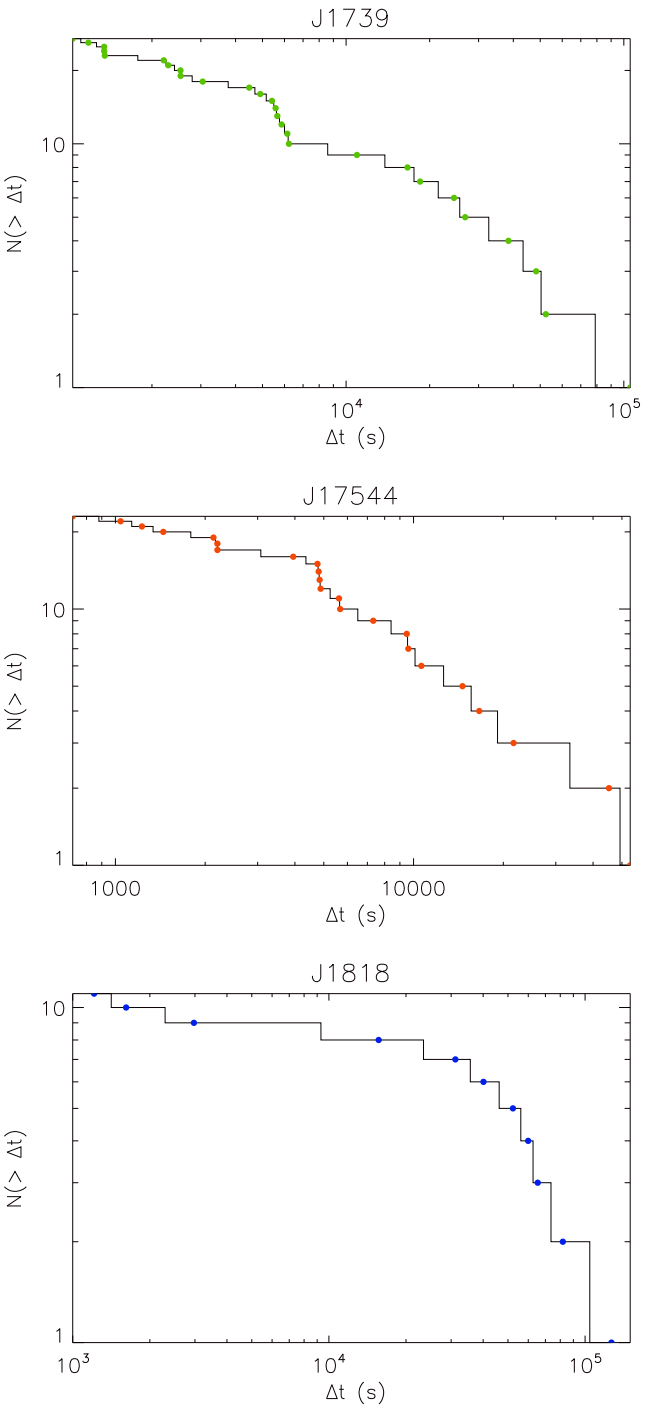

Figure 4. Cumulative distributions of elapsed times (Δt) in the three SFXTs, as observed by *INTEGRAL*/IBIS (17–50 keV).

for $D_{\rm all}$ (above ∼2 ks) and $\Delta t_{\rm all}$ (above ∼6 ks), respectively. A roll-over is present at higher time-scales (above ∼10 ks for the overall durations $D_{\rm all}$, while above ∼30–40 ks in the distribution of all elapsed times $\Delta t_{\rm all}$). The overall regular shape of the two plots is suggestive of the fact that we are seeing the same phenomenology at work in the three sources, as if to say that by merging the results from the three prototypical SFXTs, we are observing a single SFXT with a broader coverage, where almost no time-scale is missed due to observability gaps.

3.2 The energy released in the outburst versus its duration

The procedure of separation of individual outburst (a collection of physically connected flares) from the *INTEGRAL* data outlined above enables us to study their different statistical properties. In Fig. 6, we plot the total energy released in the j-th outburst, ΔE_j, as a function of its total duration, ΔT_j. In Fig. 6 the total energy is reported in units of erg (left-hand panels) and of total IBIS/ISGRI counts (17–50 keV; right-hand panels), to clearly show that the main

Downloaded from https://academic.oup.com/mnras/article-abstract/457/4/3693/2589033 by guest on 06 May 2020

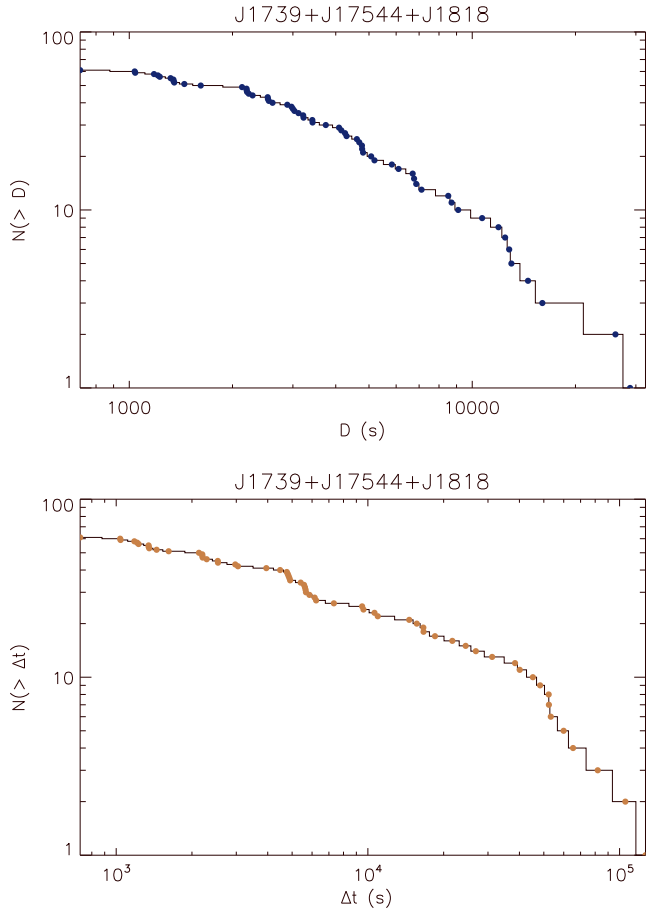

Figure 5. Cumulative distributions of the durations ($D_{\rm all}$, upper panel) and elapsed times ($\Delta t_{\rm all}$, lower panel) obtained from combining all outbursts observed from all the three SFXTs analysed here.

contribution to the uncertainty is the source distance (see PS14 for details on conversion factors from counts to physical units).

Here, $\Delta E_j = \sum_{i=1}^{N_j} \delta t_i f_i$ which is the total energy released during the j-th outburst, δt_i is the duration of i-th flare in the outburst (which was taken to be the duration of an *INTEGRAL* ScW) and f_i is the mean luminosity (erg s^{-1}) of a single flare (using a 'bin time' of one 'ScW').

In this plot, ΔT_j is the outburst duration (in the sense of the 'elapsed time' interval Δt shown in Fig. 4). It should be taken into account that the shortest ΔT_j (2000 s and shorter) are actually the durations of a single ScW, when the 'outburst' detected by *INTEGRAL* is composed by a single flare.

It is seen from Fig. 6 (summarized also in Fig. 7) that there is a correlation between the energy released in the outburst and its duration. We will discuss this correlation below.

4 DISCUSSION

For this study, we have used the *INTEGRAL*/IBIS data set of three SFXTs reported by PS14: SAX J1818.6−1703, IGR J17544−2619, and XTE J1739−302. We characterized the temporal properties of these flares calculating the WT between SFXT flares, the duration of the outburst phase as observed at hard X-rays by *INTEGRAL*, and the elapsed times between the first and the last flare belonging to the same outburst. We have observed a clustering of bright flares with WTs less than ∼1 d, which was later used to quantify the effective duration of a bright phase of an 'outburst'. Finally, we have calculated the cumulative distribution of these time-scales (durations and elapsed times) of all outbursts from all three SFXTs, finding a power-law-like behaviour.

In PS14, we concentrated on the cumulative distributions of the hard X-ray luminosity of a sample of SFXTs, compared to other three HMXBs, while Shakura et al. (2014) compared distribution of energy of SFXTs flares with the quasi-spherical settling accretion model, suggesting that the reconnection of magnetic fields carried out by stellar wind from OB-supergiants can be the physical mechanism able to trigger the opening of the NS magnetosphere, causing the sudden accretion of the captured matter, and producing the X-ray flare.

The observed cumulative distributions of temporal properties of the outbursts in three well-studied SFXTs with power-law shapes suggest possible self-similar character of the stellar wind properties in these sources, regardless the different orbital periods. It can be shown that such properties naturally arise in the frame of the model for bright SFXT flares suggested in Shakura et al. (2014). We remind that the key feature of the model is the settling accretion regime on to a slowly rotating magnetized NS (Shakura et al. 2012, 2015). This regime can set in if the X-ray luminosity from the NS is below a few times 10^{36} erg s^{-1}. At this stage, a hot convective shell is formed around slowly rotating NS magnetosphere, and the plasma entry to the NS magnetosphere is mediated by plasma cooling (Compton at higher accretion rates and radiative at low accretion rates). We argued that at the quiescent stage of SFXTs the accretion rate on to the NS is $\dot{M}_a \simeq \dot{M}_B f(u)_{\rm rad}^{1/3}$, where $\dot{M}_B$ is the standard Bondi–Hoyle–Littleton mass accretion rate (determined by the surrounding wind density ρ_w and velocity v_w) and $f(u)_{\rm rad} \sim 0.03$–0.1 is the reduction factor due to radiation plasma cooling. A magnetized stellar wind from the optical OB supergiant companion was proposed as trigger for an SFXT flare due to reconnection of large-scale magnetic field carried by the wind (Shakura et al. 2014). It was shown that the magnetic reconnection preferably occurs at small $f(u)$, which exactly corresponds to low states of SFXTs. At higher $f(u)$ and, hence, higher plasma entry rate into magnetosphere, the reconnection time is higher than the plasma magnetospheric entry time due to instabilities, so the magnetic field is admixed with plasma; this may cause additional X-ray variability with temporal properties different from what is observed, for example, in steady-state accreting X-ray pulsars like Vela X−1 (Fürst et al. 2010; PS14). During each flare initiated by the appearance of open field magnetic lines due to reconnection, the entire mass of the shell around the magnetosphere is accreted on to NS over a time interval corresponding to the free-fall time form the outer boundary of the shell (around the Bondi gravitational capture radius $R_B \approx 2GM/v_w^2$), typically of the order of 1000 s.

In this picture, the SFXT outburst is represented by a chain of flares which are physically connected to one large region of magnetized stellar wind. Therefore, the temporal properties of flares in the outburst should bear information about the magnetized wind structure. Solar wind studies suggest (Zelenyi & Milovanov 2004) that the equatorial magnetized wind agglomerates into a fractal structure with the Hausdorff dimension of $d_f \approx 4/3$, i.e. the mass inside the region of size l grows as $M_l \sim l^{d_f}$. In the context of the present study, the size of the magnetized stellar wind region is related to the duration of the outburst, $l \sim \Delta t \times v_w$, where $v_w \sim 1000$ km s^{-1} is the typical stellar wind velocity. Therefore, Fig. 5 suggests that the longest outbursts $\sim 10^5$ s correspond to the largest size of the magnetized wind clouds of about 100 $R_\odot$, which is commensurable to the orbital separation in these sources.

Downloaded from https://academic.oup.com/mnras/article-abstract/457/4/3693/2589033 by guest on 06 May 2020

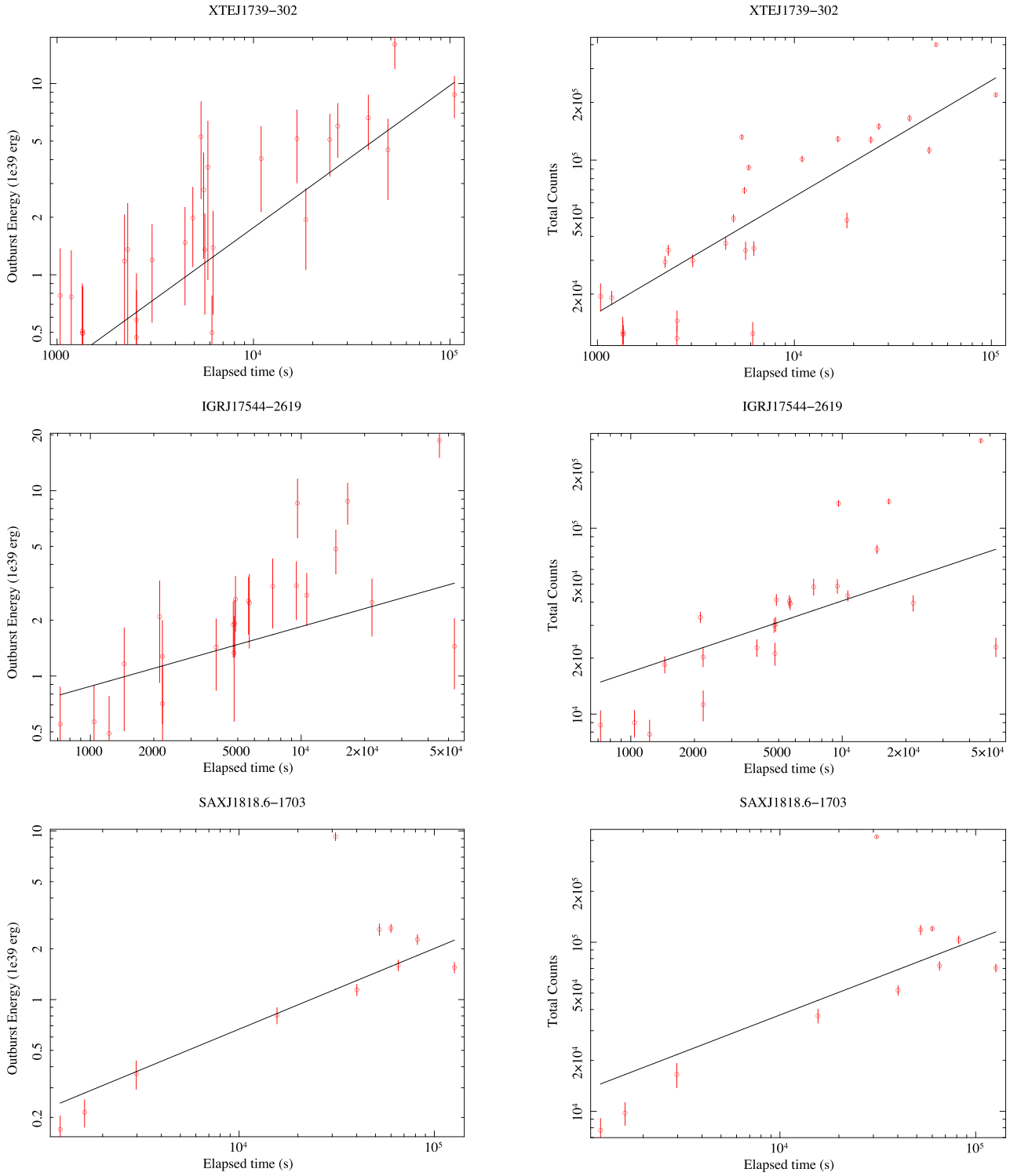

Figure 6. Power-law fits to the outburst energy (17–50 keV) versus elapsed times Δt (i.e. outburst duration, as defined in the text) of the three SFXTs. On the left the panels showing the best-fitting power law to the energy versus elapsed times, on the right the best-fitting power law to the IBIS/ISGRI counts versus elapsed times. Large uncertainties are mainly due to the large uncertainty on the source distances ($\pm$1 kpc in XTE J1739−302 and IGR J17544−2619; $\pm$0.1 kpc in SAX J1818.6−1703).

The gravitational capture (Bondi) radius R_B for the typical wind velocity from O-supergiants $\sim$1000 km s^{-1} is about 2×10^{10} cm, much smaller than the orbital separation. Therefore, during an outburst of duration Δt, the volume of the wind captured by NS is $\Delta V_0 \sim R_B^2 \times v_w \times \Delta t$. Suppose this volume to contain N clumps with some mass distribution (which is actually not important for our purposes). We stress once again here, while several authors in previous literature have discussed the possibility of direct accretion of wind clumps in SFXTs (e.g. Walter & Zurita Heras 2007), we adopt here the completely different scenario of settling accretion.

Downloaded from https://academic.oup.com/mnras/article-abstract/457/4/3693/2589033 by guest on 06 May 2020

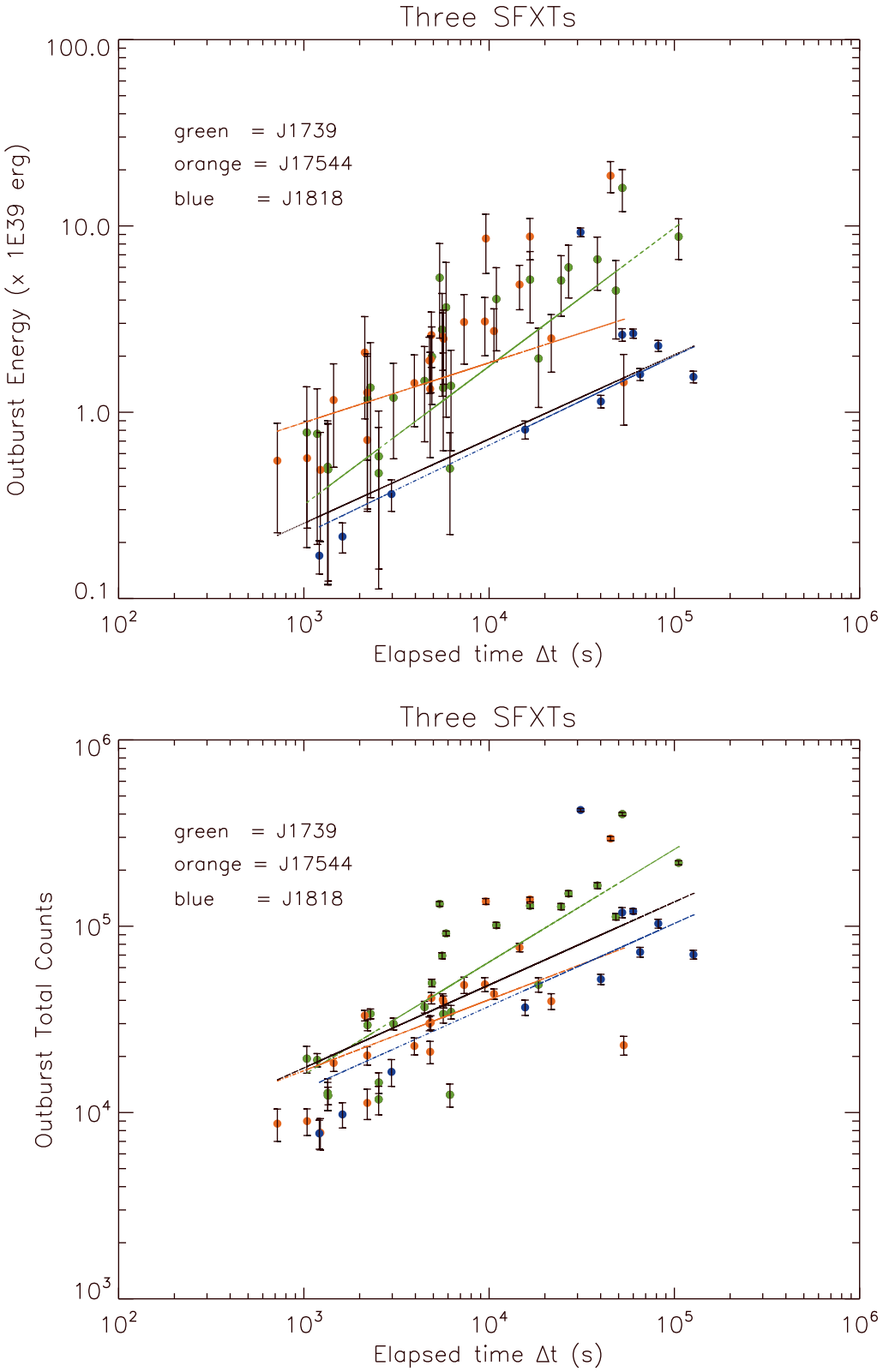

Figure 7. Summary plots of the power-law fits (in the upper panel the best-fitting power law to the energy versus elapsed times in different colours, in the lower panel the best-fitting power law to the IBIS/ISGRI counts versus elapsed times). The thin black line marks the power-law fit to the data set of the three sources combined.

Downloaded from https://academic.oup.com/mnras/article-abstract/457/4/3693/2589033 by guest on 06 May 2020

This means that not only the wind dense clumps, which are present at all times, are responsible for the SFXT activity, but their special properties (e.g. temporarily ejected magnetized lamps of the O-supergiant clumpy wind) are needed to trigger SFXT outbursts. The mass in the clumps is $\Delta M = \sum_{i=1}^{N} \rho_i V_i$, where ρ_i and V_i is the density and volume of the i-th clump, respectively. Assume the mean clump density ρ_1 for all clumps, which is much larger than the density of the surrounding wind. Then the total mass within the volume V_0 reads $\Delta M \approx \rho_1 \sum_{i=1}^{N} V_i$, neglecting the interclump mass. Therefore, the average density of the wind is $\bar{\rho}_w = \Delta M / V_0$. In the case of the magnetized wind, as we mentioned, during an outburst the magnetospheric instability due to reconnection effectively leads to the Bondi accretion regime, i.e. we expect that the total mass accreted on to NS in the entire outburst should be around ΔM. As the accreted mass corresponds to the total energy ΔE released in the outburst, it is expected that

$$\Delta E \propto \bar{\rho}_w \Delta t \,. \tag{1}$$

If the wind has a fractal structure, i.e. the density in the wind volume increases as $\bar{\rho}_w \propto l^{d_f - 3}$, taking into account the relation $l \sim v_w \Delta t$, we find

$$\Delta E \propto \Delta t^{d_f - 2} \,. \tag{2}$$

Clearly, in the case of homogeneous (on average, although maybe clumpy) wind density with $d_f = 3$ the linear dependence of the released energy on the outburst duration, $\Delta E \sim \Delta t$ is expected. Note that here we assumed a constant wind velocity, which seems to be reasonable in so far as the duration of the even longest outburst is much smaller than the orbital period of the binary system. If we take into account the possible additional wind acceleration between the companion and the NS location, the power-law index in the above relation $\Delta E \sim \Delta t^b$ will increase: $b > d_f - 2$.

Equation (2) suggests a pure observational test of the wind structure, which can be performed in two ways.

First, in each particular source, the energy released may be written as

$$\Delta E = \sum_{i=1}^{N} \dot{M}_i \Delta t_i = \langle \dot{M} \rangle D \,, \tag{3}$$

where $\langle \dot{M} \rangle$ is the mean accretion rate in the flares, which, we remind, in the Bondi accretion regime is determined solely by the density, ρ_1, and velocity, v_w, of captured matter (clearly, actually observed variations in $\dot{M}_i$ in particular flares reflect variations in density of the corresponding blob being accreted). Comparing with equation (2), we find the relation

$$D \propto \Delta t^{d_f - 2} \,, \tag{4}$$

which includes only observed quantities. Again, in the case of on average homogeneous wind with $d_f = 3$, a linear dependence is expected. In Fig. 8, we plot these relation for three SFXTs under study (the straight line marks linearity in the three cases).

As it is unclear how to estimate errors in D and Δt, it is not possible to perform a formal fit to the data. However, we note that in the worst case, on the y-axis the error on the 'D'values could reach 10 per cent at most, while on the x-axis each elapsed time Δt_i is, in the worst case, constrained in the range [Δt_i, Δt_i+1 d], by definition. Therefore, it is clearly seen that non-linearity appears

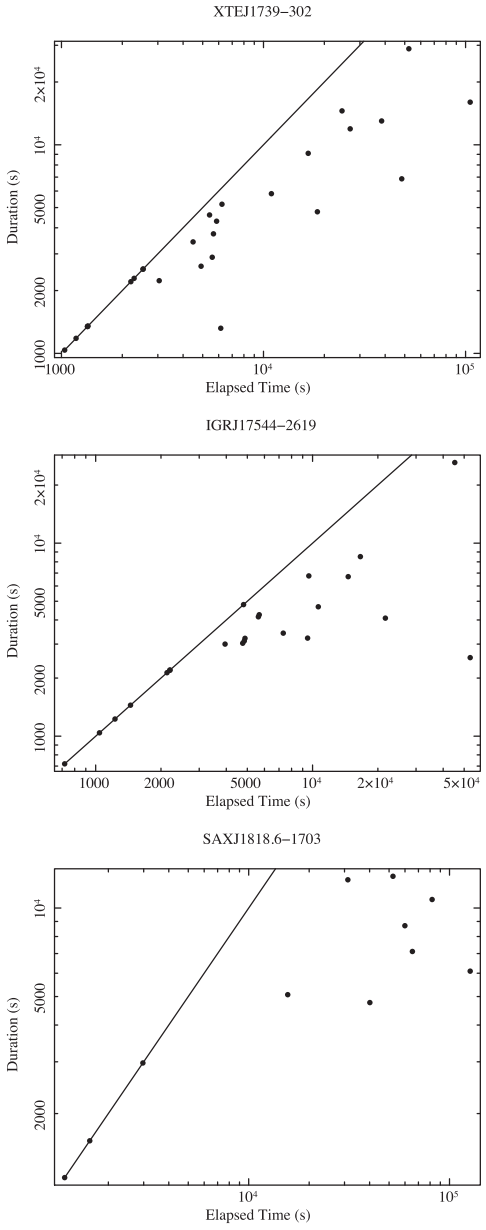

Figure 8. Total duration of outburst (D) versus elapsed times Δt (i.e. outburst duration, as defined in the text) of the three SFXTs. The straight line marks $D = \Delta t$.

with increasing outburst duration, in all sources.[1] This is indeed expected, since deviations from homogeneity for (physical) fractal structures are more prominent on large scales.

Obviously, increase in the outburst statistics would allow a more precise statistical analysis.

The second way to test equation (2) is to directly compare the energy released in each outburst with its duration.

Comparison with the observed correlation (see Fig. 6 and Table 1) shows that, on average, $b \approx 0.5$, implying $d_f - 2 < 0.5$ and hence $d_f < 2.5$ for stellar winds in the studied SFXTs. This suggests a fractal structure of the OB-supergiant winds accreting on to NS in these sources. Of course, the radiatively driven winds from

[1] The strictly linear behaviour for $Dt < 3000$ s correspond to the 'outbursts' consisting of isolated flares, as mentioned in Section 3, for which $Dt = D$ by definition.

Downloaded from https://academic.oup.com/mnras/article-abstract/457/4/3693/2589033 by guest on 06 May 2020

Table 1. Results obtained fitting the outburst energy (or total IBIS/ISGRI counts in the energy band 17–50 keV) versus the outburst duration (Elapsed time) with a power-law model, defined as $y = ax^b$. Quoted uncertainties are at 1σ.

Source	Norm a	Pow slope b	χ^2 (dof)
Counts versus Elapsed time			
XTE J1739−302	244 ±17	0.606 ±0.007	2912.0 (25)
IGR J17544−2619	1210^{+140}_{-110}	0.38 ±0.01	2386.0 (21)
SAX J1818.6−1703	620 ±80	$0.44^{+0.02}_{-0.01}$	615.1 (9)
All sources	800 ±40	0.446 ±0.004	9637.0 (59)
Energy versus Elapsed time			
XTE J1739−302	$0.0019^{+0.0020}_{-0.0010}$	0.74 ±0.08	29.40 (25)
IGR J17544−2619	$0.10^{+0.06}_{-0.04}$	0.32 ±0.06	60.70 (21)
SAX J1818.6−1703	$0.0082^{+0.0019}_{-0.0016}$	0.48 ±0.02	403.0 (9)
All sources	0.011 ± 0.002	0.45 ±0.02	582 (59)

OB-supergiants should have different properties than the solar wind, but the appearance of fractal structures in magnetized plasma flows seems very plausible.

In the proposed picture, the matter is gravitationally captured by the NS and is stored in the shell around the magnetosphere until the reconnection of the captured magnetic field occurs. The duration of refilling the magnetospheric shell by gravitationally captured matter should occur on the same time-scale as the flare itself (of the order of the free-fall time from the Bondi radius, a thousand of seconds), which leads to a continuous sequence of flares during the entire time of the outburst due to accretion of magnetized clump of stellar wind. The observed nearly power-law distribution of durations of SFXT outbursts reflects the size distribution of magnetized clouds in the wind of the OB-supergiant companions.

Clearly, an increased statistics of the flares and outbursts from SFTXs as well as spectroscopic observations in other bands are needed to understand properties of the magnetized winds from OB-supergiants more in depth.

Finally, it is interesting to note that the behaviour of the three prototypical SFXTs discussed here during the bright phase of their outbursts is very similar, irrespective of the wide range of orbital periods covered (∼5, 30, and 51 d; PS14; Walter et al. 2015), likely due to both the intrinsic wind properties and to the mediating role of the shell above the NS magnetosphere, in the settling accretion scenario.

5 CONCLUSIONS

We have performed a characterization of the temporal properties of X-ray flares from the three most extreme SFXTs, as observed by *INTEGRAL* in the energy band 17–50 keV, obtaining more insights into the physics producing their outbursts.

Calculating the cumulative distribution of WTs between the X-ray flares, we were able to identify the typical time-scale that clearly separates different outbursts, each composed by several single flares at ∼ks time-scale. This selection allowed us to calculate the energy emitted during SFXT outbursts, finding an interesting correlation with the outburst duration.

In the framework of the quasi-spherical settling accretion we have discussed here, the outburst properties (total emitted energy, duration and their positive correlation) carry signatures of the magnetized wind structure of the companion: an SFXT outburst is composed by a chain of X-ray flares physically connected to one large region of magnetized stellar wind that triggers the NS magnetospheric instability by means of magnetic reconnection.

The power-law slope of the correlation between total emitted energy and duration of the SFXT outbursts can be explained by the fractal structure of the OB-supergiant winds, reflecting the size distribution of magnetized clouds in the wind of the OB-supergiant companions.

ACKNOWLEDGEMENTS

Based on observations with *INTEGRAL*, an ESA project with instruments and science data centre funded by ESA member states (especially the PI countries: Denmark, France, Germany, Italy, Spain, and Switzerland), Czech Republic and Poland, and with the participation of Russia and the USA. This work has made use of the *INTEGRAL* archive developed at INAF-IASF Milano, http://www.iasf-milano.inaf.it/~ada/GOLIA.html. LS and AP acknowledge the Italian Space Agency financial support *INTEGRAL* ASI/INAF agreement no. 2013-025.R.0, and the grant from PRIN-INAF 2014, 'Towards a unified picture of accretion in High Mass X-Ray Binaries' (PI: Sidoli). The work of KP is partially supported by RFBR grant 14-02-00657. We thank the anonymous referee whose suggestions helped improve and clarify the manuscript.

REFERENCES

Bozzo E., Falanga M., Stella L., 2008, ApJ, 683, 1031
Bozzo E., Romano P., Ducci L., Bernardini F., Falanga M., 2015, Adv. Space Res., 55, 1255
Ducci L., Sidoli L., Mereghetti S., Paizis A., Romano P., 2009, MNRAS, 398, 2152
Fürst F. et al., 2010, A&A, 519, A37
Grebenev S. A., Sunyaev R. A., 2007, Astron. Lett., 33, 149
in't Zand J. J. M., 2005, A&A, 441, L1
Lutovinov A. A., Revnivtsev M. G., Tsygankov S. S., Krivonos R. A., 2013, MNRAS, 431, 327
Negueruela I., Smith D. M., Reig P., Chaty S., Torrejón J. M., 2006, in Wilson A., ed., Proc. of the 'The X-ray Universe 2005'. (ESA SP-604). 26–30 September 2005, El Escorial, Madrid, Spain, p. 165
Negueruela I., Torrejón J. M., Reig P., Ribó M., Smith D. M., 2008, AIPC, 1010, 252
Paizis A., Sidoli L., 2014, MNRAS, 439, 3439 (PS14)
Paizis A., Mereghetti S., Götz D., Fiorini M., Gaber M., Regni Ponzeveroni R., Sidoli L., Vercellone S., 2013, Astron. Comput., 1, 33
Romano P. et al., 2014a, A&A, 562, A2
Romano P., Ducci L., Mangano V., Esposito P., Bozzo E., Vercellone S., 2014b, A&A, 568, A55
Romano P. et al., 2015, A&A, 576, L4
Sguera V. et al., 2005, A&A, 444, 221
Shakura N., Postnov K., Kochetkova A., Hjalmarsdotter L., 2012, MNRAS, 420, 216
Shakura N., Postnov K., Sidoli L., Paizis A., 2014, MNRAS, 442, 2325
Shakura N. I., Postnov K. A., Kochetkova A. Y., Hjalmarsdotter L., Sidoli L., Paizis A., 2015, Astron. Rep., 59, 645
Sidoli L., Romano P., Mereghetti S., Paizis A., Vercellone S., Mangano V., Götz D., 2007, A&A, 476, 1307
Sidoli L. et al., 2008, ApJ, 687, 1230
Sunyaev R. A., Grebenev S. A., Lutovinov A. A., Rodriguez J., Mereghetti S., Gotz D., Courvoisier T., 2003, The Astron. Telegram, 190, 1
Walter R., Zurita Heras J., 2007, A&A, 476, 335
Walter R., Lutovinov A. A., Bozzo E., Tsygankov S. S., 2015, A&AR, 23, 2
Zelenyi L. M., Milovanov A. V., 2004, Phys.-Usp., 47, 1

This paper has been typeset from a TEX/LATEX file prepared by the author.

Downloaded from https://academic.oup.com/mnras/article-abstract/457/4/3693/2589033 by guest on 06 May 2020